2. Methods

2.3 CIMS

Experiments utilizing the bisulfate/sulfate buffer (IO3-5, IO8, SW3-5, SW8, and CL1) sometimes exhibited cyclical CIMS signal changes for Br_2 (*m/z* 285, 287, 291), IBr (*m/z* 333, 335) with no attributable cause. These signal changes occurred seemingly at random and to varying extents. In Fig. S1a, Experiment IO4 (pH = 1.7, includes H_2O_2) demonstrates the most extreme example of this behaviour that almost appears to affect the analysis. First at t = -3, the Br_2 rises briefly before falling. Then at t=2, the Br_2 signal begins to resemble a sine wave. All data beyond t=2 is not considered for this specific experiment. In Fig S1b, the effect during Experiment SW5 (pH = 1.7, includes H_2O_2) is more muted, beginning at approximately t = -6 for IBr and Br_2. As represented by these figures, this behaviour being farther away from our periods of integration is typical of the remaining experiments. Because these signal changes occurred outside of the experimental periods analyzed (i.e., before irradiation, and after O_3 had been active for one hour), they are therefore not believed to affect our results and their interpretation.

3. Results

3.1 Dark reaction production of I_2

In cases without OH precursors at pH < 2, significant photochemical I_2 production still occurs (integrated production of 14 ± 10 nmol for IO8, and 6.0 ± 2.0 nmol for SW8), while Br_2 and Cl_2 concentrations remain below limits of detection (consistent with Abbatt et al., (2010), in which no Br_2 was observed without an OH-precursor) (Table 2, main text). This production likely stems from the mechanisms outlined by Kim et al. (2016) (R13-14, R10-R12), discussed in the Sect. 1. As discussed in Sect. 3.1, H_2O_2 or NO_2^- can react directly with I^-, thereby reducing the available [I^-] for photochemical OH oxidation when pH < 2. When H_2O_2 was the oxidant, integrated I_2 production amounts were found to be ≤ 0.82 nmol (IO4, IO5, and SW5), likely due to this initial dark depletion. When instead NO_2^- is used (as in IO3 and SW3),

initial amounts of I_2 on flowtube connection to CIMS were less than when H_2O_2 was used (Table S1, Fig. S3). To estimate how much I^- may have been lost from our frozen sample by these dark mechanisms, we convert the integrated I_2 production amounts from Table S1 to I^- (by multiplying by 2) and subtract from the maximum possible moles of I^- in our samples (0.0800 L * 1.6 x 10^{-6} M = 1.28 x 10^{-7} moles I^-). For the samples that use hydrogen peroxide, as little as 36– 91% of I^- is available for reaction, while 94-97% remain when using NO_2^-. However, it is certain that not all of the I_2 produced by this mechanism went into the CIMS by the nature of having to break the flow tube seal in order to connect it to the CIMS, and so these are only estimates that could be affected by the length of time the tube is open to the environment and not connected to the CIMS, or sealed shut.

3.2 Hydroxyl radical-induced halogen production at pH ≈ 4.7

Considering the values of I_2 production from Table 2 (main text), IO2, appears to have produced ~10 times less I_2 based on the chosen period of integration. It was noted that I_2 appeared to already be present within the flow tube on connecting the flow tube to the CIMS (Fig. S2). This production could possibly be induced by room light during the transfer of the flow tube from the cooling box to the experimental light box. However, this is believed to be minimal relative to the production from the solar simulator bulbs in the photolysis box; the relative absorption spectrum for hydrogen peroxide ceases significant absorption above 400 nm (Phibbs and Giguère, 1951), while the emission spectrum of typical fluorescent lights begins significant emission above 400 nm. However, the experiment otherwise eventually produces the same qualitative features as the other three experiments after light activation (Fig. S2). If instead the limits of integration are chosen starting when the I_2 signal begins rising (i.e., during a period that qualitatively resembles the other experiments), the integrated I_2 production amounts (1.1 ± 0.6 nmol) more closely resemble the aforementioned experiments. In these conditions and in the time span of the experiment, relatively little Br_2 was produced (maximum of 34 ± 2 pmol, experiment IO2), and Cl_2 concentrations remained below limits of detection.

3.4 Effects of O_3 on halogen production

As discussed in the main text, HOX compounds were observed when O_3 was added to the flow tube. With regard to the extent to which it affects our observed signal, we believe volatile organic compounds, such as aldehydes and ketones, that may form gas phase HX could originate from our cylinder of zero air. However, we believe this source would be effectively scrubbed by our activated charcoal trap (Fig. 1), mitigating any gas phase production of HX. There also exists organic matter in the condensed phase, averaging 70 mg/L in each Instant Ocean sample (Sect. 2 of the main text). This carbon-matter is presumably uncharged and would freeze throughout the formed ice (i.e., no freeze concentration effect), therefore making only a small fraction of the total carbon available at the frozen surface for reaction.

If any of this solution-based carbon were involved in making HX, it would be expected that the SW and IO experiments produce different amounts of $IOHX^-$, given that the SW experiments were found to average ~5 mg/L of dissolved organic matter. However, there is no difference in the signal changes between corresponding SW and IO experiments (Figs. 3-4, S3). Therefore, we believe the primary source of $IOHX^-$ in the CIMS is, indeed, HOX formed in the flow tube.

4. Discussion

Through flow tube experiments involving condensed phase hydroxyl radical production, I^-, Br^-, and Cl^- were oxidized to produce I_2, Br_2, and Cl_2, respectively, from frozen saline surfaces. At low pH (~2), and with H_2O_2 as our OH precursor, we noted a large outflux of I_2 on connecting the flow tube to the CIMS. Br_2 production was readily observed in the presence of light, and enhanced when the samples were exposed to O_3, as in Fig 2b. However, experiment SW3 (Fig. S4), which was performed with NO_2^- as the hydroxyl radical precursor, exhibited photochemical I_2 production on the introduction of radiation. Only after the introduction of O_3 was Br_2 observed (under proper isotope ratios).

In most cases, it was also found that extending limits of integration beyond 1 h after addition of O_3 did not produce I_2 in amounts that exhausted the supply of I^-. In an example experiment (IO2, Fig. S5), the limits of integration were extended to t = 15 hours after the initiation of lights. While the signal appeared

to stabilize below the I_2 LOD of 9 pmol mol^{-1}, the calculated I_2 production amount of 70 nmol for this extended integration period only accounts for 46% of the 152 total nmol of I^- available. When repeated for the other experiments at pH = 4.7, it is found that at least 16% of the original I^- remains unreacted after similarly extended limits of integration. This suggests that all of the I^- in our frozen samples may not be completely excluded to the disordered interface, and may exist within the ice bulk or inaccessible brine channels throughout the ice, and that differences in integration production amounts can originate from differences in I^- distribution during freezing (Bartels-Rausch et al., 2014; Malley et al., 2018).

References

Abbatt, J., Oldridge, N., Symington, A., Chukalovskiy, V., McWhinney, R. D., Sjostedt, S. and Cox, R. A.: Release of Gas-Phase Halogens by Photolytic Generation of OH in Frozen Halide−Nitrate Solutions: An Active Halogen Formation Mechanism?, J. Phys. Chem. A, 114(23), 6527–6533, doi:10.1021/jp102072t, 2010.

Bartels-Rausch, T., Jacobi, H.-W., Kahan, T. F., Thomas, J. L., Thomson, E. S., Abbatt, J. P. D., Ammann, M., Blackford, J. R., Bluhm, H., Boxe, C., Domine, F., Frey, M. M., Gladich, I., Guzmán, M. I., Heger, D., Huthwelker, T., Klán, P., Kuhs, W. F., Kuo, M. H., Maus, S., Moussa, S. G., McNeill, V. F., Newberg, J. T., Pettersson, J. B. C., Roeselová, M. and Sodeau, J. R.: A review of air–ice chemical and physical interactions (AICI): liquids, quasi-liquids, and solids in snow, Atmos Chem Phys, 14(3), 1587–1633, doi:10.5194/acp-14-1587-2014, 2014.

Malley, P. P. A., Chakraborty, S. and Kahan, T. F.: Physical Characterization of Frozen Saltwater Solutions Using Raman Microscopy, ACS Earth Space Chem., doi:10.1021/acsearthspacechem.8b00045, 2018.

Phibbs, M. K. and Giguère, P. A.: Hydrogen Peroxide and Its Analogues: Iii. Absorption Spectrum of Hydrogen and Deuterium Peroxides in the Near Ultraviolet, Can. J. Chem., 29(6), 490–493, doi:10.1139/v51-058, 1951.

Tables

Table S1: Integrated I_2 production amounts prior to irradiation or addition of O_3 from low pH experiments involving samples with an OH precursor. The period of integration was chosen to be immediately after connection of flow tube to the CIMS until sample was irradiated. Average LODs for I_2 across experiments was 9 ± 2 pmol mol^{-1}. "IO#" represents samples composed of Instant Ocean, and "SW#" represents "saltwater" samples, composed of reagent salts.

Experiment	Oxidant	pH	I_2 produced (nmol)	Integration time (hours)	Estimated Percent of I^- remaining for reaction
IO3	NO_2^-	2.0	4.0(±0.1)	0.55	93.7
SW4	NO_2^-	2.2	2.5(±0.1)	0.43	96.1
SW3	NO_2^-	1.8	2.0(±0.1)	0.83	96.8
IO4	H_2O_2	1.7	41(±14)	7.28	36.2
IO5	H_2O_2	1.7	5.7(±1.9)	2.92	91.1
SW5	H_2O_2	1.8	41(±14)	4.95	35.5

Table S2: Integrated I_2 produced from pH = 4.7 experiments involving samples with an OH precursor. The period of integration begins at sample irradiation and extends past the limits of analysis used in the main text. Average LODs for I_2 across experiments was 9 ± 2 pmol mol^{-1}. "IO#" represents samples composed of Instant Ocean, and "SW#" represents "saltwater" samples, composed of reagent salts.

Experiment	Oxidant	pH	I_2 produced (nmol)	Integration time (hours)	Estimated Percent of I^- remaining for reaction
IO1	H_2O_2	4.7	31(±10)	30	59
IO2	H_2O_2	4.7	35(±20)	15	54
SW1	H_2O_2	4.7	63(±23)	23	17
SW2	H_2O_2	4.5	63(±20)	17	16

Figures

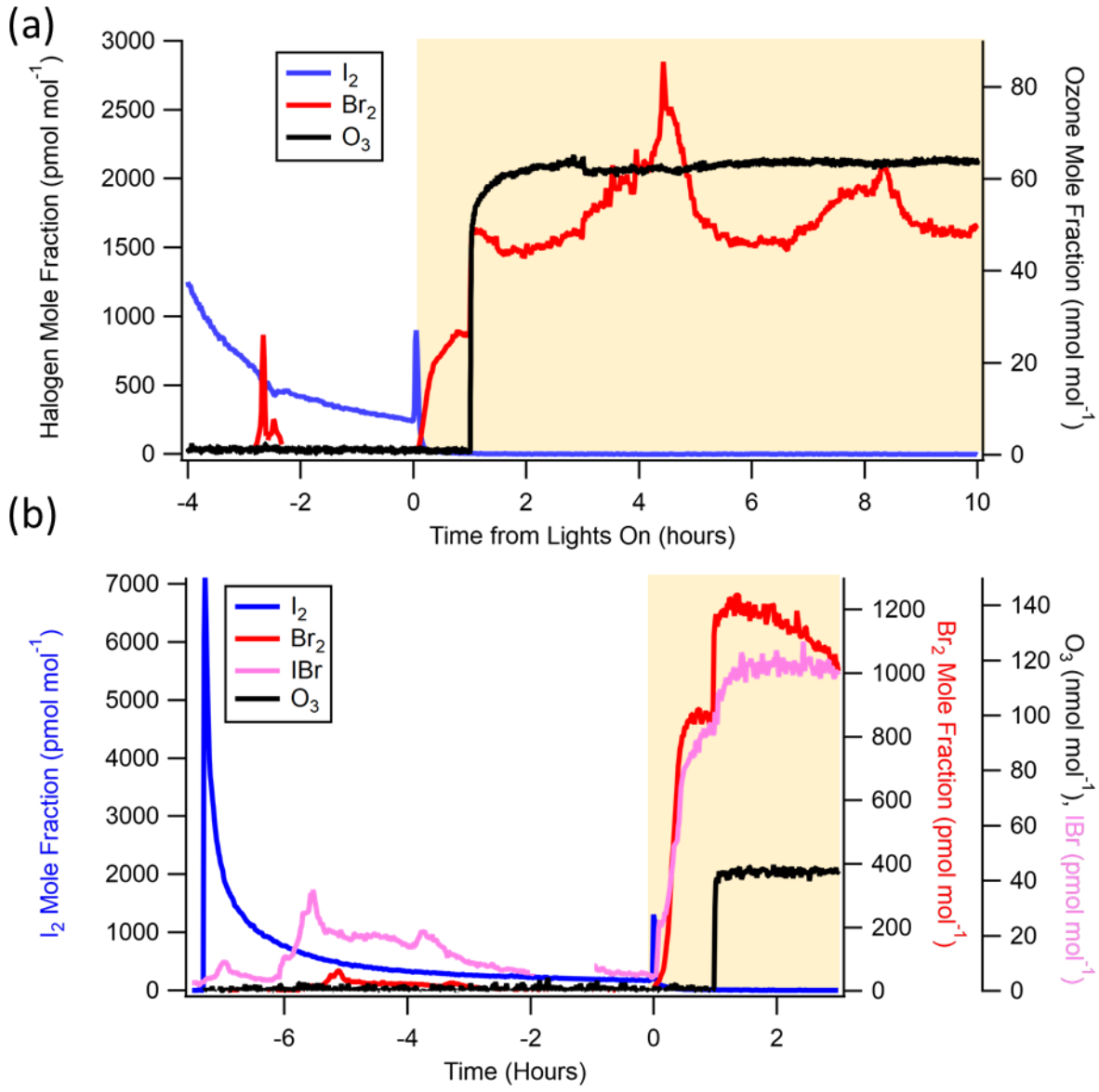

Figure S1: a) Experiment IO4 (pH < 2, includes H_2O_2) time series demonstrating cyclical increases in signal Br_2 signals, especially at t= -3 and beginning again at t = 2. Period of analysis in main text includes t = 0 until t=2. b) Experiment SW5 (pH < 2, includes H_2O_2) time series demonstrating cyclical signals for IBr and Br_2, beginning predominately at t = -6 until shortly before t = 0.

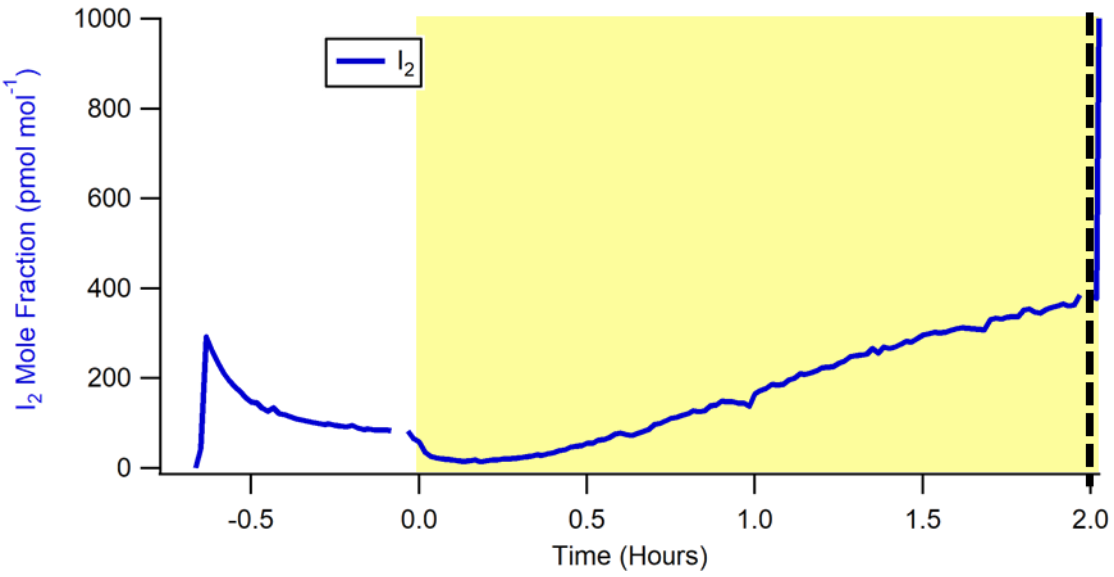

Figure S2: Experimental timeseries for experiment IO2. The key difference between this experiment and others at pH ~4.68 is that there was some initial I_2 present when the flow tube was connected to the CIMS. On activating the lights, these concentrations lowered, before ultimately rising due to OH-induced I_2 production. Beginning the integration when the signal begins rising leads to similar production values as those experiments without this initial I_2 present. Vertical dashed line represents when O_3 was introduced to the system.

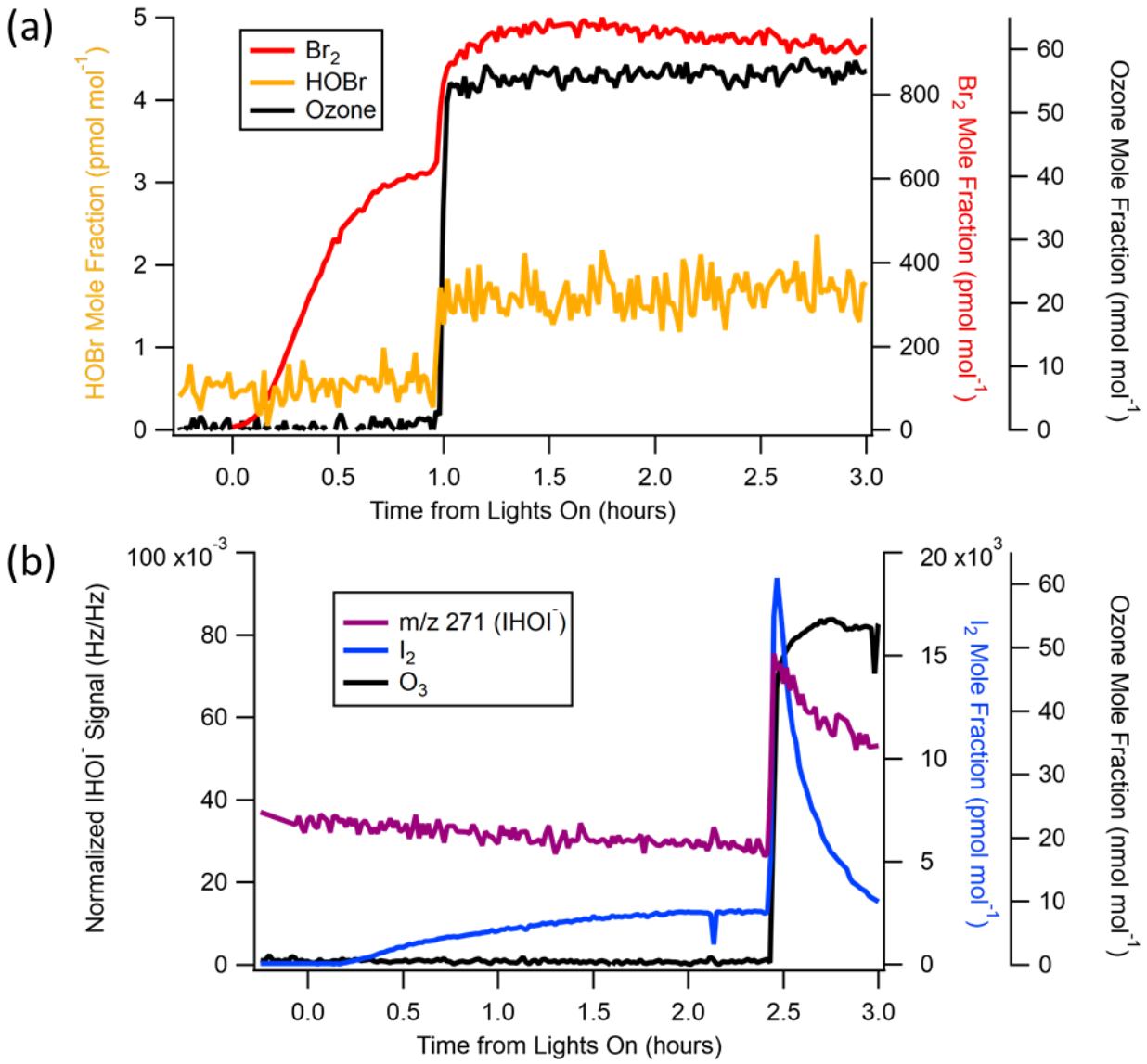

Figure S3: a) Experiment IO5, using Instant Ocean at pH = 1.7, in which H_2O_2 acted as our hydroxyl radical precursor (analogous to SW5, Fig. 4). Comparison of Br_2 mole fractions to HOBr. Note that the HOBr signal, while calibrated, should be used only for qualitative purposes as its identity could not be confirmed using isotopic ratios with *m/z* 223 due to its relatively large background signal. Br_2 data filtered based on correctness of isotope ratios between *m/z* 285 and 287 ($IBrBr^-$). b) Experiment SW2 (analogous to IO2, Fig. 3) showing effect of O_3 on I_2 and HOI.

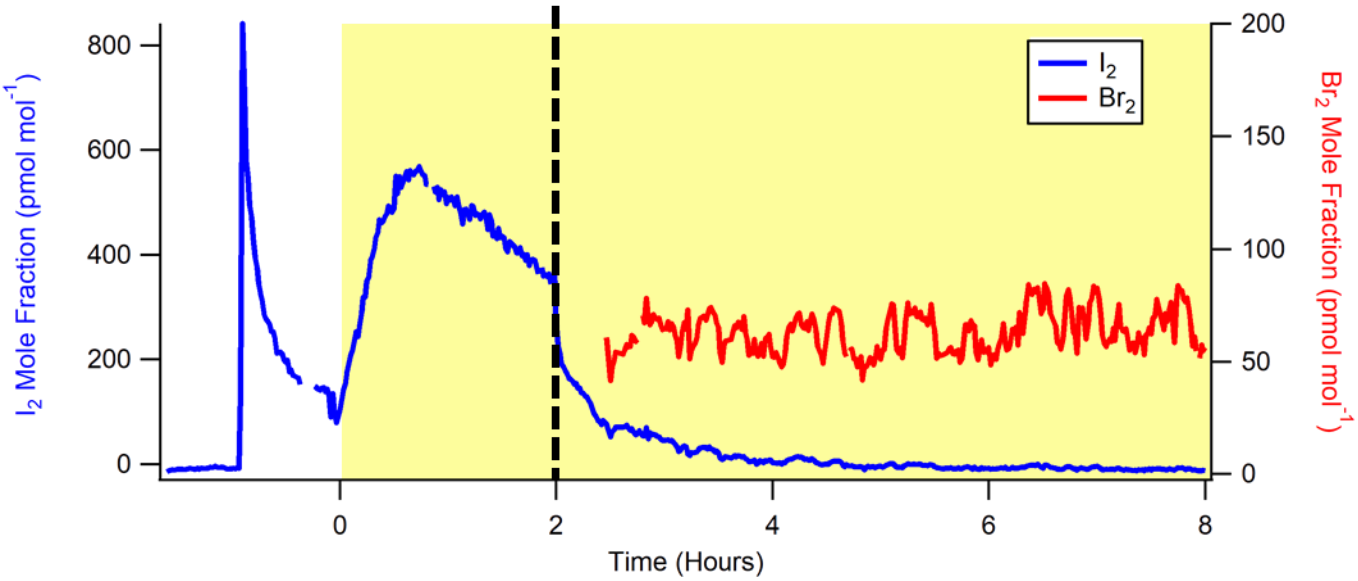

160

161 Figure S4: Experiment SW3, using synthetic seawater at pH = 1.8, in which NO_2^- acted as our hydroxyl
162 radical precursor. Ozone was introduced at hour two (indicated by dashed vertical line), coincident with
163 the I_2 concentration decrease. Br_2 data filtered based on correctness of isotope ratios between *m/z* 285 and
164 287 (IBrBr).

165

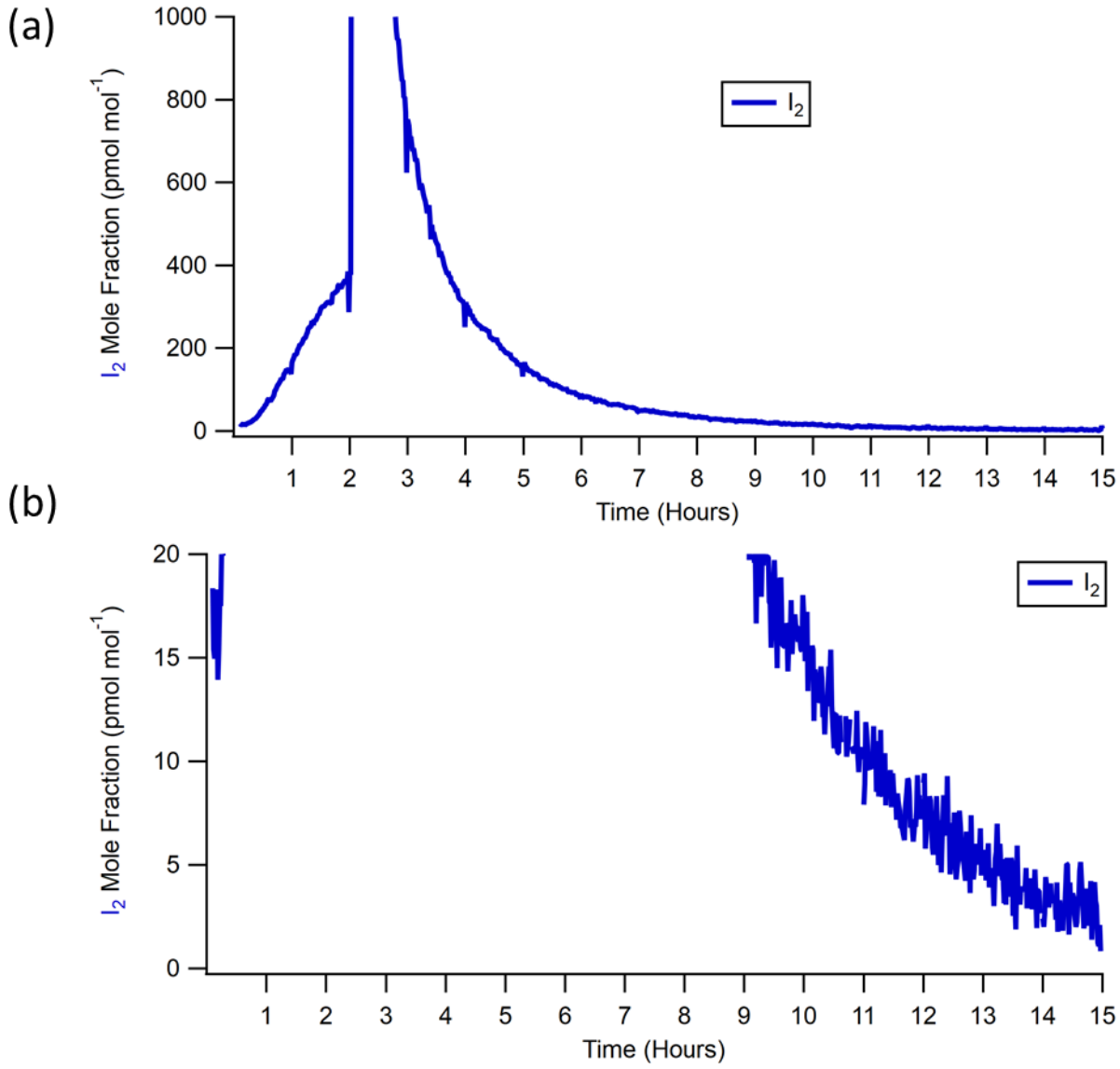

Figure S5: Iodine time series from experiment IO2, using Instant Ocean at pH = 4.7, in which H_2O_2 acted as our hydroxyl radical precursor. The x-axis begins on light introduction to the flow tube, while ozone was introduced at hour two as indicated by the sudden increase in signal. (a) The time series signal rapidly increases at t=2 coincident with the addition of 60 nmol mol^{-1} of O_3, and then returns to baseline by hour 13. (b) Zoomed in version of the same plot